ELSEVIER

Powder Technology 100 (1998) 137–146

POWDER TECHNOLOGY

Scale effects in fluidized multiphase reactors

R. Krishna *, J.M. van Baten, J. Ellenberger

Department of Chemical Engineering, University of Amsterdam, Nieuwe Achtergracht 166, 1018 WV Amsterdam, Netherlands

Received 10 November 1997; received in revised form 5 February 1998

Abstract

It is shown that the two-phase model for bubbling gas–solid fluidized beds can be extended to bubble column slurry reactors operating in the heterogeneous flow regime by proper definition of the 'dilute' and 'dense' phases. The 'dilute' phase in a bubble column slurry reactor is to be identified with the fast-rising 'large' bubbles. The 'dense' phase consists of the slurry phase in which 'small' bubbles are finely dispersed. With the aid of extensive experimental data obtained in columns of 0.1, 0.19 and 0.38 m diameter it is shown that the rise velocity of the 'dilute' phase for gas–solid fluid beds and slurry reactors show analogous scale dependencies and can be modelled in a similar manner. It is also demonstrated that fluidized multiphase reactors can be modelled in a common manner using Computational Fluid Dynamics (CFD) within the Eulerian framework. It is concluded that CFD is an invaluable tool for scaling up of fluidized multiphase reactors.

Keywords: Gas–solid fluidized bed; Computational fluid dynamics; Slurry reactors; Scale up; Two-phase model

1. Introduction

Fluidized bed and bubble column slurry reactors are finding increasing use in industrial practice; these two reactor technologies figure prominently in processes for converting natural gas to liquid fuels and light olefins [29]. There are considerable reactor design and scale-up problems associated with these natural gas conversion technologies; these problems arise because of several special features of these processes. Firstly, large gas throughputs are involved, necessitating the use of large diameter reactors, typically 5–8 m, often in parallel. Secondly, the processes operate under high pressure conditions, typically 10–80 bar. Thirdly, in order to obtain high conversion levels, large reactor heights, typically 20–30 m tall, are required. Finally, most of these processes are exothermic in nature, requiring heat removal by means of cooling tubes inserted in the reactor. Successful commercialization of natural gas conversion technologies are crucially dependent on the proper understanding of the scaling up principles of fluid beds and slurry bubble columns because these conditions fall outside the purview of most published theory and correlations [10,16].

The aim of the present paper is to provide a unified scale up philosophy for fluidized multiphase reactors, in particular gas–solid fluidized beds and bubble column slurry reactors, relying on hydrodynamic analogies between these two reactor types. We shall present evidence to underline the equality in Fig. 1. We further aim to show that both types of reactors portrayed in Fig. 1 are amenable to a similar modeling approach using Computational Fluid Dynamics (CFD) within an Eulerian framework.

2. Gas solid fluid beds: scale effects

The experimental work was carried out in three columns made of polyacrylate sections. The column diameters were 0.1 m, 0.19 m and 0.38 m with total heights of 3 or 4 m. Sintered plate gas distributors were used in these three columns. Two-stage cyclones were used to recover entrained

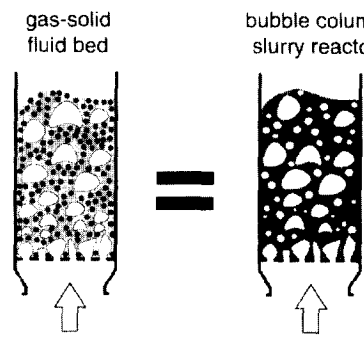

Fig. 1. Gas–solid fluid beds and bubble column slurry reactors are analogous.

* Corresponding author. Tel.: +31-20-525-7007; Fax: +31-20-525-5604; E-mail: krishna@chemeng.chem.uva.nl

0032-5910/98/$ - see front matter
PII S0032-5910(98)00134-X

fine particles and return these to the column. In all cases the pressure at the top of the column was close to atmospheric pressure. The gas inlet pipe at the bottom of the column was equipped with a quick shut-off valve for the purpose of performing dynamic gas disengagement experiments. Air was used as the gas phase in the experiments. The solid phase consisted of fluidized cracking catalyst (FCC) ($\rho_{bulk} = 960$ kg/m^3; $\rho_p = 1480$ kg/m^3; particle size distribution: 10% <23 μm, 50% <49 μm, 90% <89 μm). The unexpanded bed height ranged from $H_0 = 0.1$ to 1.5 m. For settled bed heights exceeding 1 m, it was established that the bubbles had reached their equilibrium bubble size within a distance of 0.5 m above the distributor. The superficial gas velocity U was in the range 0.001 to 0.65 m/s.

A typical dynamic gas disengagement experiments with air–FCC in the 0.38 m diameter column is shown in Fig. 2. The initial sharp decrease in the bed height is due to escape of the fast-rising bubbles ('dilute' phase). When all the bubbles have disengaged the gas in the emulsion or 'dense' phase escapes. The slope of the second part of the curve can be used to determine the superficial gas velocity of the gas through the dense phase, U_{df}. The total gas voidage, or hold-up for G–S fluid bed was calculated from $\varepsilon = (H - \rho_{bulk} H_0/\rho_p)/H$. The gas hold-up of the 'dilute' phase, ε_b, is determined from $\varepsilon_b = (H - H_1)/H$. The gas voidage in the 'dense' phase is $\varepsilon_{df} = (\varepsilon - \varepsilon_b)/(1 - \varepsilon_b)$. For a range of gas velocities the dense phase gas voidage remains practically constant and is also independent of the column diameter. The rise velocity of the bubbles, i.e., dilute phase can be determined from $V_b \equiv (U - U_{df})/\varepsilon_b$. The bubble rise velocity data for settled bed heights greater than 1 m are shown in Fig. 3 for the three column diameters. The strong influence of the bed diameter is evident. On examination of Fig. 3 we see that the bubble rise velocity in columns of 0.1 m and 0.19 m diameter tends to reach a plateau after a certain gas velocity, a sure sign of slugging behaviour. The 0.38 m diameter column does not experience slugging behaviour.

In order to develop a model for the bubble rise velocity in a gas–solid fluid bed we first draw analogies with rise of single gas bubbles in a liquid in inviscid flow [5,7,9,17,18,43]. The influence of the column diameter on the rise velocity is taken into account by introducing a scale factor correction into the Davies–Taylor relation

$$V_b^0 = 0.71\sqrt{g d_b}(\mathrm{SF}) \tag{1}$$

where the superscript 0 is used to emphasize that the rise velocity refers to that of a single, isolated, bubble. Collins [7] has determined the scale correction factor:

$$\begin{aligned} &\mathrm{SF} = 1 && \text{for } \frac{d_b}{D_T} < 0.125 \\ &\mathrm{SF} = 1.13\exp\left(-\frac{d_b}{D_T}\right) && \text{for } 0.125 < \frac{d_b}{D_T} < 0.6 \\ &\mathrm{SF} = 0.496\sqrt{D_T/d_b} && \text{for } \frac{d_b}{D_T} > 0.6 \end{aligned} \tag{2}$$

Eqs. (1) and (2) are also valid for a single bubble rising in a gas–solid fluidized bed [5,9,18,20]. Bubbles in a smaller diameter column tend to rise slower than bubbles in a larger diameter column due to the restraining effects of the column walls. Such wall effects can be expected to diminish with increasing column diameter.

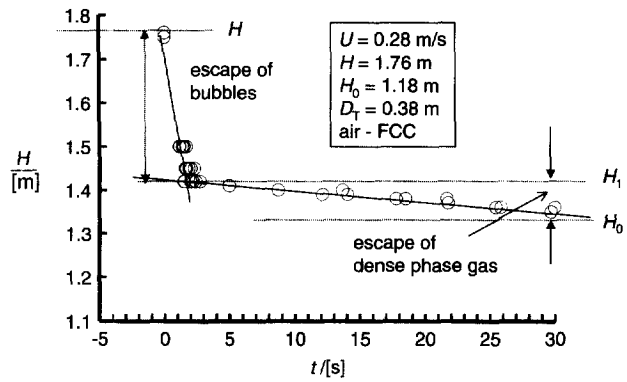

Fig. 2. Typical dynamic gas disengagement experiment for air–FCC in a 0.38 m diameter column.

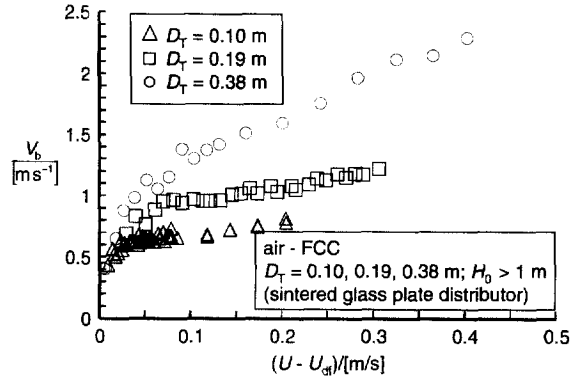

Fig. 3. Influence of superficial gas velocity through dilute phase and column diameter on the dilute phase rise velocity in gas–solid fluidized beds.

The rise velocity in a bubble swarm will be higher than that of a single gas bubble due to wake interactions [17]. A bubble which gets into the wake of a preceding bubble gets accelerated. Such acceleration effects are observed in both gas–liquid systems [4,28,34] and gas–solid systems [6]. In order to take account of such wake interaction effects we introduce a multiplying factor, AF, which is the wake acceleration factor:

$$V_b = V_b^0(\mathrm{AF}) = 0.71\sqrt{g d_b}(\mathrm{SF})(\mathrm{AF}) \tag{3}$$

The acceleration factor AF can be expected to be dependent on the average distance of separation between the bubbles; the smaller the separation the greater the acceleration effect. The average distance of separation between the bubbles decreases with increasing superficial gas velocity through the dilute phase, $U - U_{df}$, and therefore the factor AF can be expected to increase with increasing values of $U - U_{df}$. We fitted our experimental data set for V_b for the 0.1, 0.19 and 0.38 m diameter columns with the Eqs. (1)–(3) to obtain expressions for the wake acceleration factor AF and the bub-

ble size d_b. The regressed relations yielded the following expressions:

$$AF = 1.64 + 2.7722(U - U_{df}) \quad (4)$$

$$d_b = 0.204(U - U_{df})^{0.412} \quad (5)$$

The fitted acceleration factors are shown in Fig. 4 along with the measured acceleration factors from the rise velocity data. The correlation Eqs. (4) and (5) are valid for superficial gas velocities in the range 0.05 to 0.4 m/s and the scatter of the measured acceleration factors is within 15% of the fitted Eq. (4). We note that the bubble rise velocity in a gas–solid fluid bed are about 1.5 to 3 times higher than the rise velocity of a single gas bubble, given by Eq. (1), underlining the strong wake interaction effects. An examination of the acceleration factor data shows that there is no systematic deviation from the fitted line for any particular column diameter. It can therefore be concluded that the Collins scale correction factor (Eq. (2)) adequately represents the scale effects for bubble swarms in fluidized beds.

The fitted bubble size correlation (5), also shown in Fig. 4, matches extremely closely with the values calculated from the [8] bubble growth formula

$$d_b = 0.54(U - U_{df})^{2/5}(h + h_0)^{4/5} g^{-1/5} \quad (6)$$

taking the bed height h to be 0.5 m and $h_0 = 0.03$ m for porous plate distributors; see the dashed line in Fig. 4. Our experimental results can be rationalized by assuming that the bubbles reach their equilibrium bubble size at a distance 0.5 m above the distributor. In reality there is a distribution of bubble sizes and the fitted d_b represents an average value. Eqs. (1)–(5) are sufficient to allow calculation of the dilute phase rise velocity in a fluidized bed.

The two-phase model for gas–solid fluids, pictured in Fig. 5 provides a practical model for design and scale up. This two-phase model will now be shown to be applicable also to bubble column slurry reactors.

3. Bubble column slurry reactor

For natural gas conversion technologies using say the Fischer–Tropsch or methanol synthesis, the heterogeneous

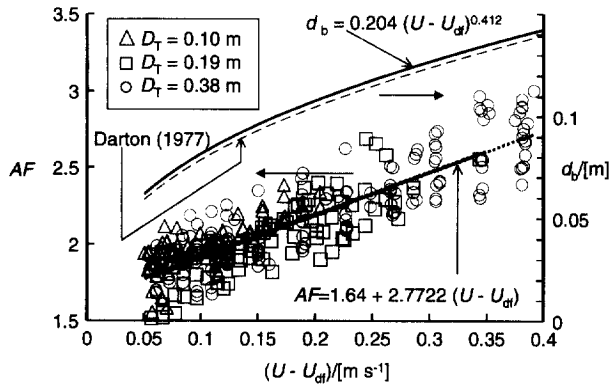

Fig. 4. Correlation for dilute phase rise velocity in gas–solid fluidized bed. Only data for unexpanded bed heights H_0 exceeding 1 m were incorporated into the fits.

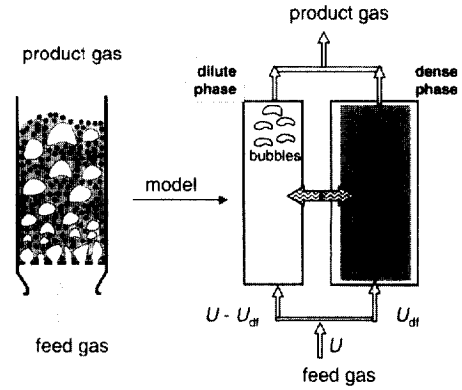

Fig. 5. Two-phase model for gas–solid fluidized bed.

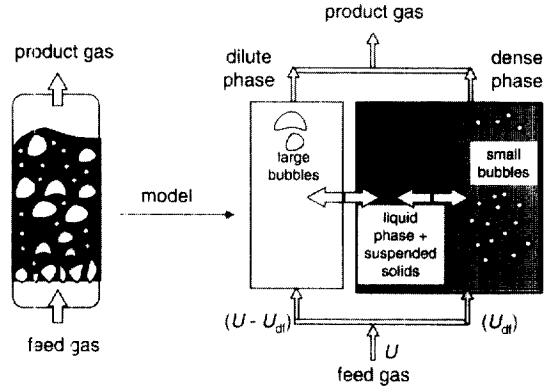

Fig. 6. Generalized two-phase model applied to a bubble column slurry reactor operating in the churn–turbulent regime.

or churn–turbulent flow regime is the preferred regime of operation [39]. In the churn–turbulent regime of operation a roughly bi-modal size distribution prevails in a bubble column slurry reactor. 'Large' bubbles, typically in the 20–50 mm range, traverse the column at high rise velocities approaching 1.5 m/s, churning up the slurry phase. 'Small' bubbles, smaller than about 5 mm, are finely dispersed in the slurry phase and have the same backmixing characteristics as the liquid phase. The two phase model can be adopted to describe the slurry bubble column hydrodynamics in the heterogeneous flow regime; see Fig. 6.

In order to verify the hydrodynamic picture in Fig. 6, experiments were performed in polyacrylate columns with inner diameters of 0.1, 0.19 and 0.38 m. The gas distributors used in the three columns were all made of sintered plates. All columns were equipped with quick closing valves in the gas inlet pipe in order to perform dynamic gas disengagement, or bed collapse experiments. Pressure taps were installed along the height of the columns. Validyne DP15 pressure sensors, connected to the pressure taps and coupled to a PC, allowed the transient pressure signals to be recorded during dynamic gas disengagement experiments. The gas flow rates entering the column were measured with the use of a set of rotameters, placed in parallel, as shown in Fig. 7 for the 0.38 m column. This set-up was typical. All experiments were performed with paraffin oil (density, $\rho_L = 790\ kg\ m^{-3}$; viscosity, $\mu_L = 0.0029$

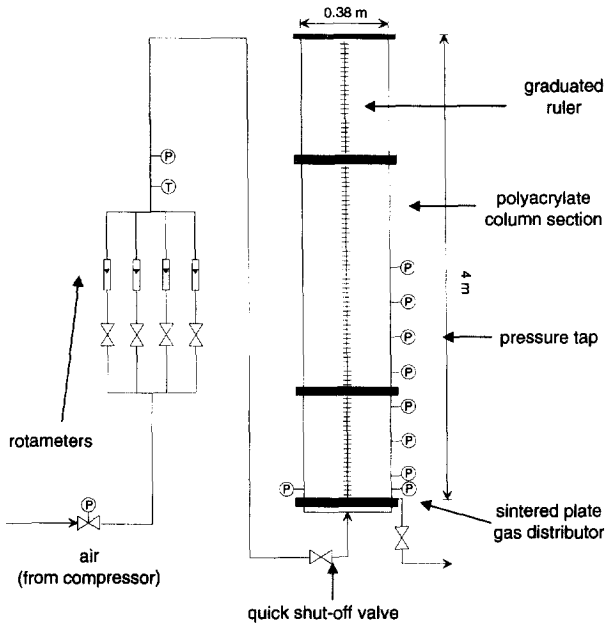

Fig. 7. Experimental set-up for the 0.38 m diameter column.

Pa s; surface tension, $\sigma = 0.028$ N m^{-1}) as liquid phase. The properties of the liquid phase were determined experimentally. Air was used as the gas phase in all experiments. The solid phase used consisted of porous silica particles whose properties were determined by experiments to be as follows: skeleton density = 2100 kg m^{-3}; pore volume = 1.05 ml g^{-1}; particle size distribution, d_p: 10% <27 μm; 50% <38 μm; 90% <47 μm. The solids concentration ε_s, is expressed as the volume fraction of solids in gas free slurry. The pore volume of the particles (liquid filled during operation) is counted as being part of the solid phase.

The influence of the solids concentration on the total gas hold-up ε for varying superficial gas velocities are shown in Fig. 8 for the 0.38 m diameter column. It is observed that increased particles concentration tends to decrease the total gas hold-up, ε, to a significant extent. This decrease in the total gas hold-up is due to the decrease in the hold-up of the small bubbles due to enhanced coalescence caused due to the presence of the small particles.

A typical dynamic gas disengagement profile for air—36 vol.% paraffin oil slurry in the 0.38 m column for the churn turbulent flow regime of operation is shown in Fig. 9. After the shut-off of the gas supply, the hold-up decreases due to the escape of fast rising 'large' bubbles ('dilute' phase). When the 'large' bubbles have escaped the 'small' bubbles leave the column. The gas voidage in the 'dense' phase, ε_{df}, is obtained as indicated in Fig. 9. The gas hold-up of the 'large' bubbles, i.e., 'dilute' phase is obtained from $\varepsilon_b = (\varepsilon - \varepsilon_{df})/(1 - \varepsilon_{df})$. Fig. 10 shows the collection of data on ε_{df} for all column diameters and slurry concentrations. We see that the dense phase gas hold-up ε_{df} is virtually independent of the column diameter and is a significant decreasing function of the particles concentration. The unique dependence of the decrease in the dense phase gas voidage ε_{df} with

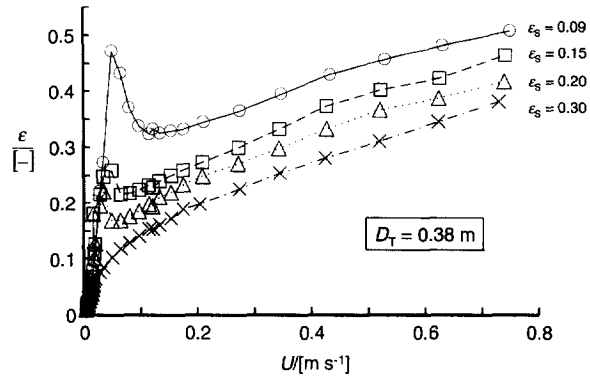

Fig. 8. Influence of increased solids concentration on the total gas hold-up for air/paraffin oil/silica in a 0.38 m diameter column.

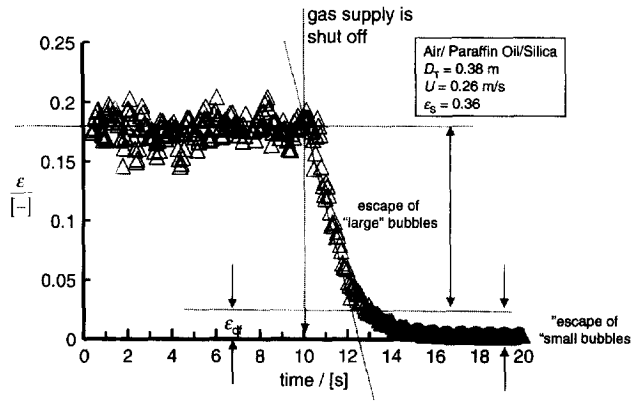

Fig. 9. Dynamic gas disengagement experiments for air/36 vol.% paraffin oil slurry in the 0.38 m diameter column.

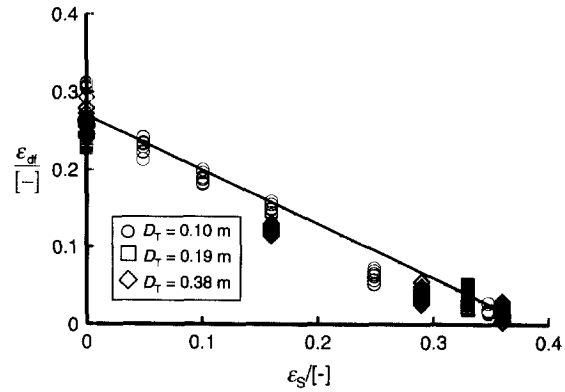

Fig. 10. Reduction in the dense phase gas hold-up with increasing solids volume fraction.

increasing solids volume fraction ε_s is useful for scale up purposes because this parameter can be determined in a relatively small diameter column under actual reaction conditions of temperature and pressure.

In Fig. 11 we compare the dilute phase gas hold-up measured for the systems air–FCC and air–slurry in the column of diameter 0.38 m with 36 vol.% catalyst. Remarkably the dilute phase gas hold-ups in these two completely different systems are almost indistinguishable from each other. To provide an explanation of the coincidence of the dilute phase

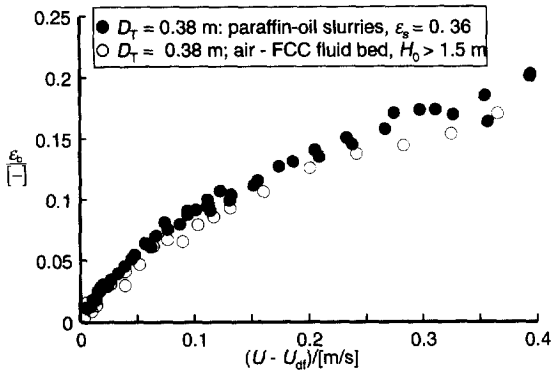

Fig. 11. Comparison of dilute phase gas hold-up in air–FCC and air–slurry systems for 0.38 m diameter column. For air–FCC only data for $H_0 > 1.5$ m are shown. For the air–slurry data only data for 36 vol.% slurry is used.

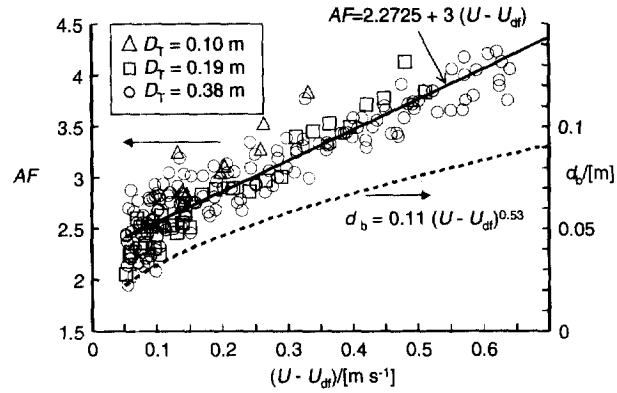

Fig. 12. Fit for rise velocity of 'large' bubbles (dilute phase) in a slurry bubble column.

gas hold-up data, we attempt to develop a correlation for the large bubble rise velocity in slurry bubble columns, obtained from $V_b \equiv (U - U_{df})/\varepsilon_b$. From an estimate of the slurry viscosities for the various concentrations used in the experiments we determined that the rise of large bubbles corresponding to inviscid flow conditions [5]. Therefore the same model Eq. (3) is expected to be applicable to describe the rise velocity of large gas bubbles in slurries. From the set of measurements of the dilute phase gas hold-up (= large bubble hold-up), ε_b, obtained in slurry bubble columns of diameters of 0.1, 0.19 and 0.38 m, with slurry concentrations varying in the range $0.16 < \varepsilon_s < 0.37$, the dilute phase rise velocities V_b were determined. The following fitted relations were obtained for the wake acceleration factor:

$$AF = 2.2725 + 3(U - U_{df}) \quad (7)$$

and the average size of the large bubble population:

$$d_b = 0.11(U - U_{df})^{0.53} \quad (8)$$

The bubble sizes calculated according to Eq. (8) are in line with the measured bubble sizes in a two-dimensional slurry bubble column [40]. The correlation Eqs. (7) and (8) are valid for superficial gas velocities in the range 0.05 to 0.65 m/s and for slurry concentrations in the range $0.16 < \varepsilon_s < 0.37$. The scatter of the measured acceleration factors is within 15% of the fitted Eq. (7). Furthermore, there is no systematic deviation between the experimentally determined acceleration factors from the fitted Eq. (7) and so we concluded that the Collins scale correction factor (2) correctly represents the scale effects for swarms of large bubbles in slurry bubble columns. A comparison of Figs. 4 and 12, shows that both the acceleration factors and the bubble sizes of the dilute phases are of comparable magnitude for fluid beds and slurry columns. It is concluded that the bubble growth mechanism in slurry bubble columns is similar to that for gas–solid fluid beds. Also, the acceleration effects caused by wake interactions are similar in these two reactor types. The numerical differences in the acceleration factors are due to the differences in the viscosity of the dense phase.

Having established the analogies between gas–solid fluid beds and bubble column slurry reactors, especially with respect to modeling of the rise velocity of the dilute phase, we now proceed to develop a common CFD model.

4. Eulerian simulations of fluidized multiphase reactors

In recent years there has been considerable academic and industrial interest in the use of computational fluid dynamics (CFD) to model gas–solid fluidized beds and bubble columns. CFD modeling of fluidized beds usually adopts the Eulerian framework for both the dilute and dense phases and makes use of the granular theory to calculate the dense phase rheological parameters [18,19,1,2,30,21,14,27,41]. The granular theory can be successfully applied for relatively coarse Geldart B powders and its extension to Geldart A powders poses several problems in respect the proper modeling of interparticle collision and interaction [19]. Discrete particle Langrangian simulations of the particle phases have also been attempted [24]. The use of CFD models for gas–liquid bubble columns has also evoked considerable interest in recent years and both Euler–Euler and Euler–Langrange frameworks have been employed for the description of the gas and liquid phases [3,11,13,22,23,26,31–33,35,37, 38,42]. A recent review [25] analyses the various modeling aspects involved for vertical bubble driven flows. Our purpose in this paper is to demonstrate how CFD model can be used for scaling up of fluidized multiphase reactors.

The two-phase model portrayed in Figs. 5 and 6 underlies our approach, wherein lumped phases 'dilute' and 'dense' are defined as shown and ascribed fluid properties. For the air–FCC system we estimate the 'dense' phase viscosity μ_{df} to be 0.125 Pa s, using the data summarized in Ref. [45]. The density of the dense phase ρ_{df} was estimated from the experimental data to be 830 kg m^{-3}. For the air–paraffin oil–silica catalyst slurry reactor with a catalyst concentration of 35 vol.%, the dense phase properties were estimated to be $\mu_{df} = 0.05$ Pa s and $\rho_{df} = 960$ kg m^{-3}. For the chosen slurry concentration of 35 vol.%, the small bubbles are virtually

destroyed and the similarities between the slurry bubble column and the gas solid fluid bed is particularly striking.

For each of the 'dilute' and 'dense' phases shown the volume-averaged mass and momentum conservation equations are given by

$$\frac{\partial \rho_k}{\partial t} + \nabla \cdot (\rho_k \boldsymbol{u}_k) = 0 \tag{9}$$

$$\frac{\partial (\rho_k \boldsymbol{u}_k)}{\partial t} + \nabla \cdot (\rho_k \boldsymbol{u}_k \boldsymbol{u}_k) = -\varepsilon_k \nabla p - \nabla \cdot (\varepsilon_k \tau_k) + \mathbf{M}_{kl} + \rho_k g \tag{10}$$

where ρ_k, $\boldsymbol{u}_k$, ε_k and τ_k represent, respectively, the macroscopic density, velocity, volume fraction and stress tensor of the kth phase, p is the pressure, $\mathbf{M}_{kl}$, the interphase momentum exchange between phase k and phase l and g is the gravitational force. Other forces such as lift, Magnus and Saffmann are ignored in the present analysis [25]. For the continuous, dense, phase, the turbulent contribution to the stress tensor is evaluated by means of $k-\varepsilon$ model, using standard single phase parameters. The dilute (bubble) phase, which is the dispersed phase, is assumed to be in laminar flow. It was also determined from CFD simulations that the assumption regarding the flow field inside the bubbles were not crucial. The momentum exchange between the dilute (subscript b) and dense (subscript df) phases is given by

$$\mathbf{M}_{df,b} = \frac{3}{4} \rho_{df} \frac{\varepsilon_b}{d_b} C_D (\boldsymbol{u}_b - \boldsymbol{u}_{df}) |\boldsymbol{u}_b - \boldsymbol{u}_{df}| \tag{11}$$

The interphase drag coefficient is calculated from

$$C_D = \frac{4}{3} \frac{\rho_{df} - \rho_G}{\rho_{df}} g d_b \frac{1}{V_b^2} \tag{12}$$

where the rise velocity of the dilute phase V_b is given by the Eq. (3). The wake acceleration factor AF and the bubble size d_b are calculated using Eqs. (4), (5), (7) and (8), respectively for fluid beds and slurry reactors. The assumption of constant bubble size along the height of the column is an important limitation and the results of the simulation are expected to apply to describe the hydrodynamics of tall commercial scale reactors with a high height to diameter ratio. Furthermore, our CFD model ignores mass transfer between the dilute and dense phases and any chemical reaction in the dense phase.

A commercial CFD package CFX 4.1c of AEA Technology, Harwell, UK, was used to solve the equations of continuity and momentum for the two-fluid mixture. This package is a finite volume solver, using body-fitted grids. The grids are non-staggered and all variables are evaluated at the cell centers. An improved version of the Rhie–Chow algorithm [36] is used to calculate the velocity at the cell faces. The pressure–velocity coupling is obtained using the SIMPLEC algorithm [15]. For the convective terms in Eqs. (8) and (9) hybrid differencing was used. A fully implicit backward differencing scheme was used for the time integration.

Three column configurations were simulated: (a) 0.19 m diameter column of 3 m height, (b) 0.38 m diameter column of 3 m height, and (c) 1.5 m diameter column of 8 m height. The initial height of the 'liquid', i.e., dense phase in the three cases (a), (b) and (c) were 1.9 m, 1.9 m and 4 m, respectively. For the 0.19 m and 0.38 m diameter columns simulations were carried out for a range of superficial gas velocities through the dilute phase, $U - U_{df}$ in the range 0.09–0.5 m/s corresponding to those used in the experiments reported earlier in this paper. For a chosen set of operating conditions and column diameter the bubble size d_b and the corresponding drag coefficient C_D was calculated using Eq. (12).

Axi-symmetry was assumed in the simulations using cylindrical coordinates. The computational grid used for the 0.38 diameter column is shown in Fig. 13. Anticipating steeper velocity gradients near the wall region and in the bottom portion of the column, a non-uniform grid was used. In the radial direction 30 grid cells were used, 10 grid cells in the central core and 20 grid cells towards the wall region. In the axial direction the first 0.2 m bottom portion of the column consisted of 10 mm cells and the remainder 2.8 m height consisted of 20 mm cells. The total number of cells was 4800. The same number of grid cells was also used for simulations of the 0.19 m diameter column. The dilute phase gas was injected only at the inner 13 of the total number of 30 cells. This injection strategy was used because the dilute phase tends to concentrate in the center of the column and the applied gas injection strategy helped achieve easier convergence. A similar computational grid strategy was used for the 1.5 m diameter column where a total of 30 750 cells were used: 75 in the radial direction and 410 in the axial direction. The computational grid used in this work is finer than the corresponding grids used in simulations of gas–liquid bubble columns by other workers [22,31,37,38,42]. The time stepping strategy used in the transient simulations for attainment of steady state was: 20 iterations at 5×10^{-4} s, 20 iterations

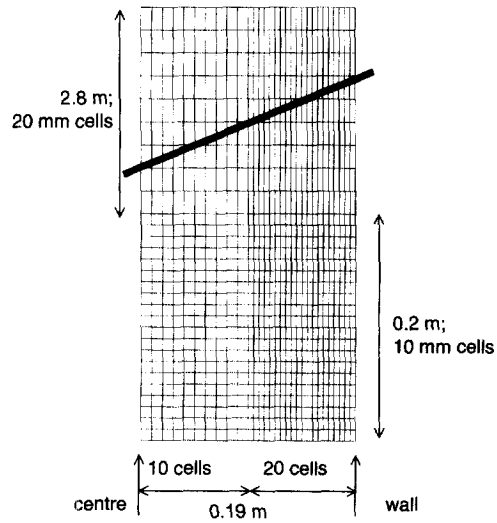

Fig. 13. Computational grid used in axi-symmetric CFD simulation of a 0.38 m diameter column.

at 1×10^{-3} s, 460 iterations at 5×10^{-3} s, 2000 iterations at 1×10^{-2} s. For any given column simulations were first carried out for the lowest value of $(U-U_{df})$ and the converged solution used as a starting guess for the simulation at a higher value of the superficial gas velocity. The 0.19 m and 0.38 m diameter column simulations were carried out on a Silicon Graphics Power Indigo workstation with the R8000 processor. Each simulation was completed in about 8 h. In all the runs steady state was reached within 1500 iterations; this is illustrated in Fig. 14 which shows the center line velocity of the dense phase at a height of 1.6 m above the distributor of the 0.38 m diameter fluid bed operating at $U-U_{df}=0.09$ m/s. The sharp change in the centre line velocity after about 500 iterations is caused by the bubble 'front' approaching the monitoring point. The 1.5 m diameter column simulations was carried out on a Silicon Graphics Power Challenge with six R8000 processors used in parallel and took about 48 h to reach steady-state.

The gas hold-up of the 'dilute' phase determined from the CFD simulations corresponded very well with the experimental data; this is demonstrated in Fig. 15 for the 0.38 m diameter fluidized bed and in Fig. 16 for the 0.19 m diameter slurry bubble column. Generally speaking the dilute phase gas hold-up calculated from the CFD simulations tend to be slightly lower than those measured. This is because in the bed collapse experiment, the influence of circulation of the dense phase tends to accelerate the bubble motion [12]. Put another way, the bed collapse experiments used to set up the drag relations tend to overestimate the bubble rise velocity.

In Fig. 17 the center line velocity of the dense phase $V_{df}(0)$ is plotted as a function of the column diameter for a range of superficial gas velocities $(U-U_{df})$ for both fluid beds and slurry columns. The differences in the center line velocity of fluid beds and slurry columns are small. With increasing column diameter there is a significant increase in the center line velocity of the dense phase. Eulerian simulations obviate the need for using a separate correlation for the center-line dense phase velocity.

The strong scale effects evidenced in Fig. 17 is further emphasized in Fig. 18 when comparing the influence of column diameter on the radial distribution of the dense phase velocity. The strong downward velocity at the wall leads to intense backmixing of the 'dense' phase.

The residence time distribution of the gas phase can also determined from the CFD simulations, after attainment of steady-state, by injection of a hypothetical gas tracer at the inlet and monitoring the response at a height of 2 m above the distributor. The dimensionless tracer concentration is shown in Fig. 19 for the fluid bed of 0.38 m diameter operating

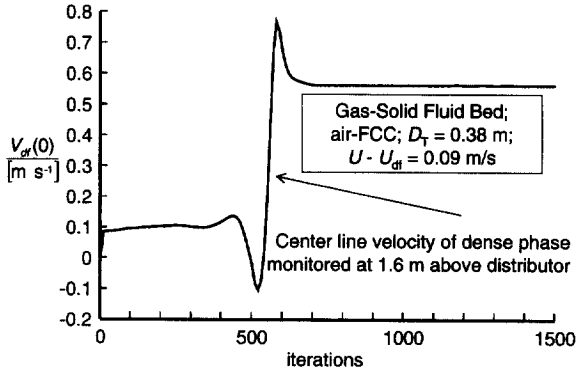

Fig. 14. Transient approach to steady state in CFD simulations of a 0.38 m fluid bed reactor operating at 0.09 m/s. The center line dense phase velocity $V_{df}(0)$, monitored at 1.6 m above the distributor is plotted against number of iterations.

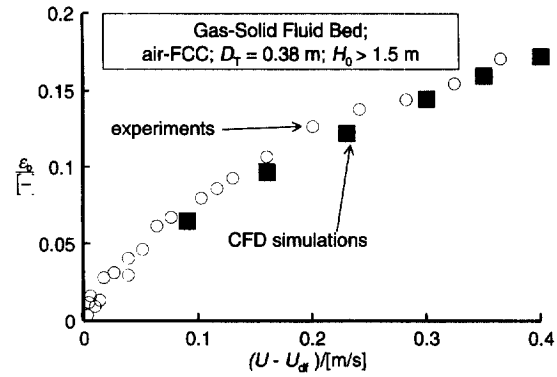

Fig. 15. The hold-up of the 'dilute' phase as a function of the superficial gas velocity through the dilute phase for 0.38 m diameter air–FCC fluid bed. Comparison of experimental data for $H_0 > 1.5$ m with CFD simulations.

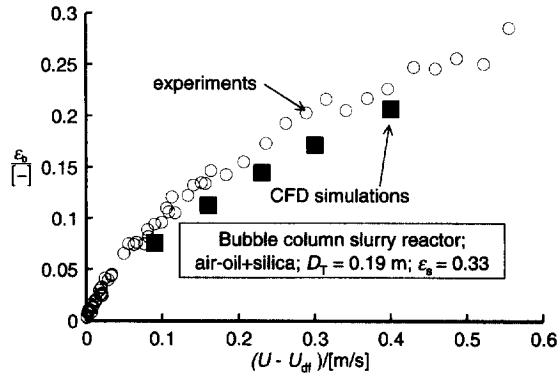

Fig. 16. The hold-up of the 'dilute' phase as a function of the superficial gas velocity through the dilute phase for 0.19 m diameter slurry bubble column. Comparison of experimental data for 33 vol.% silica concentration in paraffin with CFD simulations.

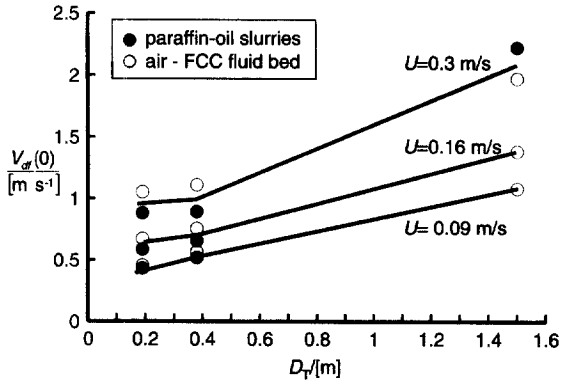

Fig. 17. The center line velocity of the 'dense' phase, $V_{df}(0)$, plotted against column diameter for a range of values of $(U-U_{df})$.

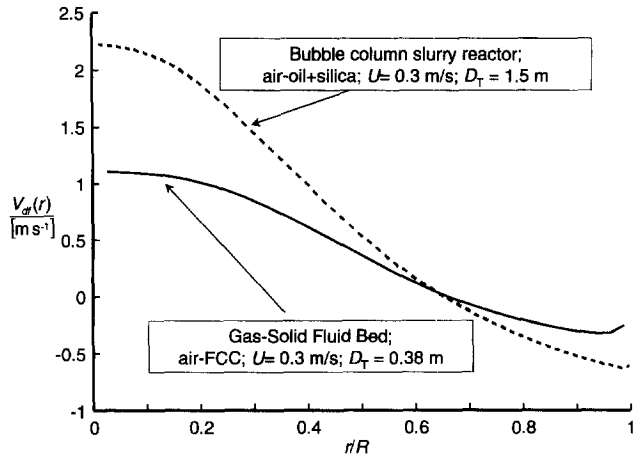

Fig. 18. The radial distribution of the axial dense phase velocity, demonstrating the strong influence of column diameter. When compared at the same values of $(U-U_{df})$, the radial distribution of the axial dense phase velocity for a fluid bed agrees with that of a slurry reactor of the same diameter.

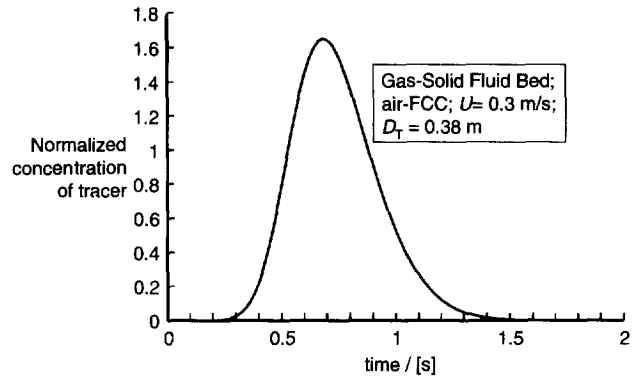

Fig. 19. The residence time distribution for the dilute phase in a fluid bed of 0.38 m diameter operating at a superficial gas velocity of 0.3 m/s. RTD obtained from tracer injection at gas inlet during CFD simulation after steady-state had been achieved.

at a velocity of 0.3 m/s. By fitting an axial dispersion model to this simulation the value of the gas phase $D_{ax,G}$ is found to be 0.114 $m^2\ s^{-1}$. For the gas–solid fluid beds and slurry bubble columns several tracer simulations were performed and the results for the axial dispersion coefficient of the gas phase are plotted in Fig. 20 as a function of the column diameter D_T. The strong scale dependence of $D_{ax,G}$ is evident. It can also be seen that there is little difference in the gas phase dispersion coefficients for fluid beds and slurry reactors. The values of the axial dispersion coefficient for the gas phase from the simulations show the same trend with column diameter as the experimental data points, as collated in Ref. [44]; see Fig. 21. The measured axial dispersion data refer to the total gas phase, present in both dilute and dense phases, whereas our simulations refer to axial dispersion only of the dilute phase (bubbles). It is therefore to be expected that the simulations of $D_{ax,G}$ will lie below the experimental values.

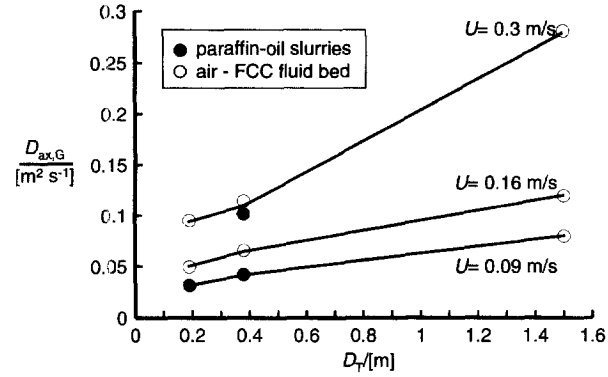

Fig. 20. Gas phase axial dispersion coefficient $D_{ax,G}$ for gas–solid fluid beds and slurry bubble columns plotted as a function of column diameter D_T.

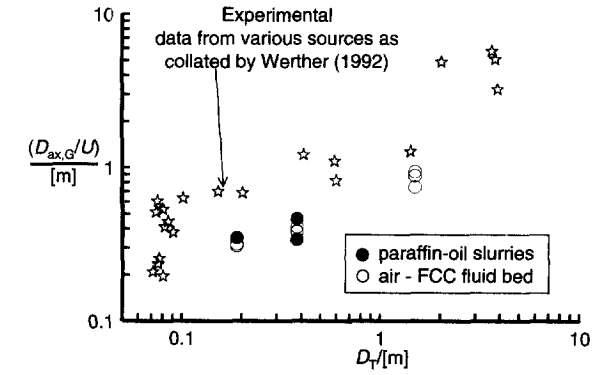

Fig. 21. Comparison of simulation results for $(D_{ax,G}/U)$ with experimental values.

5. Conclusions

The two-phase model can be used to describe the hydrodynamics of a bubble column slurry reactor by identifying the 'dilute' phase with the fast-rising 'large' bubbles. The 'dense' phase consists of the slurry phase in which 'small' bubbles are finely dispersed. We have demonstrated that the 'dilute' phase rise velocity can be correlated in an identical manner using Eqs. (1) and (2). Scale effects in fluidized multiphase reactors are shown to be analogous for fluid beds and slurry reactors.

Using the two-fluid model with estimated pseudo 'dense' phase properties, it is shown that CFD simulations of fluid beds and slurry columns can be carried out in an analogous manner. Information on the column hydrodynamics necessary for design and scale up purposes, such as gas hold-up, radial distribution of dilute and dense phase velocities, axial dispersion coefficients can be obtained with relative ease from such CFD simulations. This information is generated from information on bubble size of the dilute phase and the drag coefficient between the dilute and dense phases. The CFD simulations underline the analogies between fluid beds and slurry bubble columns.

6. Nomenclature

AF	wake acceleration factor (–)
C_D	drag coefficient defined by Eq. (8) (–)
d_b	bubble diameter (m)
d_p	mean particle size (m)
$D_{ax,G}$	axial dispersion coefficient of the gas phase ($m^2 s^{-1}$)
D_T	column diameter (m)
g	acceleration due to gravity (9.81 $m s^{-2}$)
h	height above the gas distributor (m)
h^*	height above the gas distributor where the bubbles reach their equilibrium size (m)
h_0	parameter determining the initial bubble size at the gas distributor (m)
H, H_0, H_1	height of expanded bed, ungassed bed and after escape of dilute phase (m)
M	interphase momentum exchange term
p	pressure ($N m^{-2}$)
r	radial coordinate (m)
R	radius of column (m)
t	time (s)
$\boldsymbol{u}$	velocity vector ($m s^{-1}$)
U	superficial gas velocity ($m s^{-1}$)
$(U-U_{df})$	superficial gas velocity through the dilute phase ($m s^{-1}$)
U_{df}	superficial velocity of gas through the dense phase ($m s^{-1}$)
U_{mf}	minimum fluidization velocity ($m s^{-1}$)
V_b	rise velocity of the dilute phase ($m s^{-1}$)
V_b^0	rise velocity of single gas bubble ($m s^{-1}$)
$V_{df}(r)$	radial distribution of the axial dense phase velocity ($m s^{-1}$)
$V_{df}(0)$	center line dense phase velocity ($m s^{-1}$)

Greek letters

ε	total gas voidage of G–S or G–L–S system (–)
ε_b	gas hold-up of 'dilute' phase; = 'bubbles' in G–S systems; = 'large' bubbles in bubble column slurry reactor (–)
ε_{df}	hold-up of gas in 'dense' phase; corresponds to 'small' bubble gas hold-up in bubble column slurry reactor (–)
ε_s	volume fraction of solids in slurry on gas-free basis (–)
μ_{df}	viscosity of dense phase (Pa s)
μ_L	viscosity of liquid phase (Pa s)
ρ_{bulk}, ρ_p	bulk and particle densities ($kg m^{-3}$)
ρ_{df}	density of the dense phase ($kg m^{-3}$)
ρ_G, ρ_L	density of gaseous and liquid phases ($kg m^{-3}$)
σ	surface tension of liquid phase ($N m^{-1}$)
τ	stress tensor ($N m^{-2}$)

Subscripts

ax	axial parameter
b	referring to 'dilute' or 'bubble' phase
df	referring to 'dense' phase
G	referring to gas phase
k, l	referring to k and l phases
L	referring to liquid or fluid phase
T	tower or column

References

[1] M.N. Bogere, A rigorous description of gas–solid fluidized beds, Chem. Eng. Sci. 51 (1996) 603–622.

[2] A. Boemer, H. Qi, U. Renz, Vasquez, F. Boysan, Eulerian computation of fluidized bed hydrodynamics—a comparison of physical models, Proceedings of the 13th International Conference on Fluidized Bed Combustion, Orlando, USA, 1995, pp. 775–787.

[3] N. Boisson, M.R. Malin, Numerical prediction of two-phase flow in bubble columns, International Journal of Numerical Methods in Fluids 23 (1996) 1289–1310.

[4] D. Bhaga, M.E. Weber, In-line interaction of a pair of bubbles in a viscous liquid, Chem. Eng. Sci. 35 (1980) 2467–2474.

[5] R. Clift, J.R. Grace, M.E. Weber, Bubbles, Drops and Particles, Academic Press, San Diego, 1978.

[6] R. Clift, J.R. Grace, Continuous bubbling and slugging, in: J.F. Davidson, R. Clift, D. Harrison (Eds.), Fluidization, 2nd edn., Chap. 3, Academic Press, London, 1985.

[7] R. Collins, The effect of a containing cylindrical boundary on the velocity of a large gas bubble in a liquid, J. Fluid Mech. 28 (1967) 97–112.

[8] R.C. Darton, R.D. LaNauze, J.F. Davidson, D. Harrison, Bubble growth due to coalescence in fluidized beds, Trans. Inst. Chem. Engrs. 55 (1977) 274–280.

[9] J.F. Davidson, D. Harrison, R.C. Darton, R.D. LaNauze, The two-phase theory of fluidization and its application to chemical reactors, in: L. Lapidus, N.R. Amundson (Eds.), Chemical Reactor Theory, A Review, Prentice-Hall, Englewood Cliffs, NJ, 1977, pp. 583–685.

[10] W.-D. Deckwer, Bubble Column Reactors, Wiley, New York, 1992.

[11] E. Delnoij, F.A. Lammers, J.A.M. Kuipers, W.P.M. van Swaaij, Dynamic simulation of dispersed gas–liquid two-phase flow using a discreet bubble model, Chem. Eng. Sci. 52 (1997) 1429–1458.

[12] N.S. Deshpande, N. Dinkar, J.B. Joshi, Disengagement of the gas phase in bubble columns, Int. J. Multiphase Flow 21 (1995) 1191–1201.

[13] N. Devanathan, M.P. Dudukovic, A. Lapin, A. Lübbert, Chaotic flow in bubble column reactors, Chem. Eng. Sci. 50 (1995) 2661–2667.

[14] J. Ding, D. Gidaspow, A bubbling fluidization model using the kinetic theory of granular flow, AIChE J. 36 (1990) 523–538.

[15] J. Van Doormal, G.D. Raithby, Enhancement of the SIMPLE method for predicting incompressible flows, Numer. Heat Transfer 7 (1984) 147–163.

[16] L.S. Fan, Gas–Liquid–Solid Fluidization Engineering, Butterworth, Boston, 1989.

[17] L.S. Fan, K. Tsuchiya, Bubble wake dynamics in liquids and liquid–solid suspensions, Butterworth-Heinemann, Boston, 1990.

[18] L.S. Fan, C. Zhu, Principles of Gas–Solid Flows, Cambridge Univ. Press, UK, 1998, 600 pp.

[19] G. Ferschneider, P. Mège, Eulerian simulation of dense phase fluidized beds, Revue de L'Institut Français du Pétrole 51 (1996) 301–307.

[20] D. Geldart (Ed.), Gas Fluidization Technology, Wiley, New York, 1986.

[21] D. Gidaspow, Multiphase Flow and Fluidization—Continuum and Kinetic Theory Descriptions, Academic Press, 1994.

[22] S. Grevskott, B.H. Sannæs, M.P. Dudukovic, K.W. Hjarbo, H.F. Svendsen, Liquid circulation, bubble size distributions, and

solids movement in two- and three-phase bubble columns, Chem. Eng. Sci. 51 (1996) 1703–1713.
[23] J. Grienberger, H. Hofmann, Investigations and modelling of bubble columns, Chem. Eng. Sci. 47 (1992) 2215–2220.
[24] B.P.B. Hoomans, J.A.M. Kuipers, W.J. Briels, W.P.M. Van Swaaij, Discrete particle simulation of bubble and slug formation in a two-dimensional gas-fluidized bed: a hard sphere approach, Chem. Eng. Sci. 51 (1996) 99–118.
[25] H.A. Jakobsen, B.H. Sannæs, S. Grevskott, H.F. Svendsen, Modeling of bubble driven vertical flows, Ind. Eng. Chem. Research 36 (1997) 4052–4074.
[26] H.A. Jakobsen, On the modelling and simulation of bubble column reactors using a two-fluid model, Dr.Ing. Thesis, The University of Trondheim, The Norwegian Institute of Technolgoy, Department of Chemical Engineering, Trondheim, 1993.
[27] J.T. Jenkins, S.B. Savage, A theory for the rapid flow identical, smooth, nearly elastic spherical particles, J. Fluid Mech. 130 (1983) 187–202.
[28] I. Komasawa, T. Otake, M. Kamojima, Wake behaviour and its effect on interaction between spherical-cap bubbles, J. Chem. Eng of Japan 13 (1980) 103–109.
[29] R. Krishna, J. Ellenberger, S.T. Sie, Reactor development for conversion of natural gas to liquid fuels: a scale up strategy relying on hydrodynamic analogies, Chem. Eng. Sci. 51 (1996) 2041–2050.
[30] J.A.M. Kuipers, K.J. van Duijn, F.P.H. van Beckum, W.P.M. van Swaaij, A numerical model of gas-fluidized beds, Chem. Eng. Sci. 47 (1992) 1913–1924.
[31] S. Kumar, W.B. Vanderheyden, N. Devanathan, N.T. Padial, M.P. Dudukovic, B.A. Kashiwa, Numerical simulation and experimental verification of gas–liquid flow in bubble columns, in: Industrial Mixing Fundamentals With Applications, AIChE Symposium Series No. 305, Vol. 91, 1995, pp. 11–19.
[32] A. Lapin, A. Lübbert, Numerical simulation of the dynamics of two-phase gas–liquid flows in bubble columns, Chem. Eng. Sci. 49 (1994) 3661–3674.
[33] T.J. Lin, J. Reese, T. Hong, L.S. Fan, Quantitative analysis and computation of two-dimensional bubble columns, AIChE J. 42 (1996) 301–318.
[34] S. Narayanan, L.H.J. Goossens, N.W.F. Kossen, Coalescence of two bubbles rising in a line at low Reynolds numbers, Chem. Eng. Sci. 29 (1974) 2071–2082.
[35] V.V. Ranade, Flow in bubble columns: some numerical experiments, Chem. Eng. Sci. 47 (1992) 1857–1869.
[36] C.M. Rhie, W.L. Chow, Numerical study of the turbulent flow past an airfoil with trailing edge separation, AIAA J. 21 (1983) 1525–1532.
[37] A. Sokolichin, G. Eigenberger, Gas–liquid flow in bubble columns and loop reactors: Part I. Detailed modelling and numerical simulation, Chem. Eng. Sci. 49 (1994) 5735–5746.
[38] A. Sokolichin, G. Eigenberger, A. Lapin, A. Lübbert, Direct numerical simulation of gas–liquid two-phase flows. Euler/Euler versus Euler/Lagrange, Chem. Eng. Sci. 52 (1997) 611–626.
[39] J.W.A. De Swart, R. Krishna, S.T. Sie, Selection, design and scale up of the Fischer Tropsch slurry reactor, in: M. de Pontes, R.L. Espinoza, C.P. Nicolaides, J.H. Scholtz, Natural Gas Conversion IV, Proceedings of the 4th International Natural Gas Conversion Symposium, Kruger Park, South Africa, 19–23 November 1995, Studies in Surface Science and Catalysis, Vol. 107, Elsevier, Amsterdam, 1997, pp. 213–218.
[40] J.W.A. De Swart, R.E. Van Vliet, R. Krishna, Size, structure and dynamics of 'large' bubbles in a 2-D slurry bubble column, Chem. Eng. Sci. 51 (1996) 4619–4629.
[41] M. Syamlal, T.J. O'Brien, Computer simulation of bubbles in a fluidized bed, AIChE Symposium Series 85 (270) (1989) 22–31.
[42] R. Torvik, H.F. Svendsen, Modelling of slurry reactors. A fundamental approach, Chem. Eng. Sci. 45 (1990) 2325–2332.
[43] G.B. Wallis, One-Dimensional Two-Phase Flow, McGraw-Hill, New York, 1969.
[44] J. Werther, Fluidized-bed reactors, in: B. Elvers, S. Hawkins, G. Schulz (Eds.), Chapter in Ullmann's Encyclopedia of Industrial Chemistry, 5th edn., Vol. B4, Principles of Chemical Reaction Engineering and Plant Design, VCH Verlagsgesellschaft, Weinheim, 1992.
[45] J.G. Yates, Effect of temperature and pressure on gas–solid fluidization, Chem. Eng. Sci. 51 (1996) 167–205.